A deployable and inflatable robotic arm concept for aerospace applications

A deployable and inflatable robotic arm concept for aerospace applications

Pierpaolo Palmieri
Department of Mechanical and Aerospace Engineering
Politecnico di Torino
Turin, Italy
pierpaolo.palmieri@polito.it

Matteo Gaidano
Department of Mechanical and Aerospace Engineering
Politecnico di Torino
Turin, Italy
matteo.gaidano@polito.it

Mario Troise
Department of Mechanical and Aerospace Engineering
Politecnico di Torino
Turin, Italy
mario.troise@polito.it

Laura Salamina
Department of Mechanical and Aerospace Engineering
Politecnico di Torino
Turin, Italy
laura.salamina@polito.it

Andrea Ruggeri
Department of Mechanical and Aerospace Engineering
Politecnico di Torino
Turin, Italy
andrea.ruggeri@studenti.polito.it

Stefano Mauro
Department of Mechanical and Aerospace Engineering
Politecnico di Torino
Turin, Italy
stefano.mauro@polito.it

***Abstract*—The interest in soft systems for space missions represents a growing trend in recent years. The development of inflatable robots, combined with the improvement of deployment mechanisms, allows to build novel lightweight and deployable robotic manipulators. In several space applications, the use of soft robots could minimize bulk and mass, reducing space mission costs. The main challenges in soft robotics are the control of the system and the exertion of high forces. In this manuscript, the concept of an inflatable manipulator with two inflatable links and three degrees of freedom is proposed. After a review about the possible materials to be used for the inflatable parts, the robot mechanical structure, the deploying strategy and the pneumatic line are presented. Then, an elastostatic approach is proposed to model the robot with the aim of developing its control. The last section shows preliminary experimental tests performed on the link prototype with the purpose to evaluate a static characterization in relation to the supplied pressure. Results suggest the validity of the adopted approach to model the system and clarify the pressure influence about the system performances. The study puts the basis for the development of the first prototype of the robotic system.**

Keywords—soft robotics, deployable structures, multibody model, kinematics, space robotics.

I. INTRODUCTION

Robots are becoming ubiquitous in industrial and structured environment and their presence in space missions is essential. The rigid structure of traditional robots allows great accuracy and, potentially, high force generation. However, rigid manipulators are heavy, and they require high payload capability if embarked on space vehicles.

The use of soft manipulators, i.e. robots built utilizing soft material, could better fit the requirements of space exploration instead, so it represents a growing trend in recent years. Their adaptability and low mass allow them to be used in a large variety of applications [1], as well as the ability to move on rough terrain, e.g. in extra-planetary environments [2] with different gravity level.

Space industry represents today one of the most fascinating field for soft robotics applications. Inflatable space structures, or 'space inflatables', are promising candidates for a wide range of space applications and their use is often a benefit [3]. As a matter of fact, in unstructured and not well-defined environments, as space ones, it is not sure that conventional rigid systems are the best choice to achieve the desired task [4]. Systems made in soft materials can be easily transported in compact and lightweight packages, and can be inflated to be deployed, when required. The deployment transformation allows to reach a state in which the structures is stable and able to carry out loads.

Main disadvantages of these systems are low force production and difficulty in the control, also because of the non-linearities induced by large deformation in the material and by multiphysical coupling. The full kinematics and dynamics of the system are complex mechanics problems, difficult to tackle. The design of soft manipulators can span along all the spectrum between totally soft and rigid structures [4]. To develop a soft robot with desired features it is necessary to find a good tradeoff, choosing the appropriate material and actuation method.

Some of the most relevant projects in this field were the Mars Pathfinder inflatable airbag landing system [5], the Inflatable Antenna Experiment (IAE) [6] and an inflatable and rigidable solar array [7]. Despite the space inflatable booms have low deployment accuracy and post-development stability [8], their use allows to obtain high packaging ratio and they are extremely lightweight compared to other deployable technologies.

Soft robotics, using deployable robotic manipulators based on soft materials, permit to resolve aerospace issues. Concerning the design, inflatable manipulators are typically gathered in two categories: continuum [9] and articulated robot. The latter can consist of inflatable links with rigid [10] or variable stiffness joints [11] and completely soft structure with soft joints [12], e.g. using pneumatic [13, 14], or tendon-driven actuators [15]. The design of a soft robot concerns its material, architecture, kind of actuation and control structure.

Soft robots and traditional robots use different mechanisms to achieve the desired pose. Conventional robots usually have motorized or cable-driven joints, allowing for finite degrees of freedom for each rigid component. However, continuum soft robots distribute deformations over their soft components allowing for theoretically infinite degrees of freedom [9].

The use of soft joints leads to more complexity in the design and stiffness control of the actuator [16]. Nevertheless, the manipulators with inflatable links can be modeled considering traditional approaches developed for flexible link arms [17], pseudo rigid bodies [18] and simplified small deflection assumptions [19]. The deployable and inflatable structures have advantages due to the low density and high storage efficiency, in space environment they must use a simple deployment mechanism.

Onboard application can also consider safe collaborative uses to help astronauts in their daily activities. Vision systems can provide safe workspace sharing [20, 21], while soft links can avoid any kind of damage in the event of an undesired impact and make possible their stowage in a limited volume when they are not used.

Historically, two main strategies have been used to design deployable systems: the first one involves mechanisms comprising interconnected bar elements [22, 23], the second strategy makes use of inflatable elements with pressure input [14]. The development of deployment mechanisms to package and deploy soft structures, ensuring its integrity [24] makes soft robots useful in hostile environments, such as the space. The inflatable deployable concept has the advantage to reduce the cost of space mission and possibility to build a very large space structures [25]. Winding and wrapping procedures are used both for space inflatable booms [26] and for soft robotic links [27] to effectively reduce the bulk of the system.

This work proposes a novel deployable and lightweight manipulator concept for space applications, consisting of a structure with two inflatable links and three rigid motorized joints. Tools or a 3 degrees of freedom wrist could be placed at the end-effector (EE) of the robot. In a previous work, load and pose estimation algorithms are proposed to calculate the inverse kinematics of the robot, considering the link deformations in relation to the supplied pressure [28]. The system involves a pneumatic line for inflation and deflation of the links. In the following, a review of the possible materials for the inflatable parts is presented; the robotic system is described, illustrating the pneumatic line, the deployment and the wrapping strategy for the robotic arm; an elastostatic approach is proposed to model the soft links and the experimental tests performed to characterize the robot are presented; in the end, results and conclusions are proposed.

II. Materials

Flexibility and low volume of packaging of inflatable structures are achieved using thin membranes of low elastic module and weight. Polymers are commonly adopted because of their flexibility and capability of pneumatic insulation. In addition, new polymeric materials with appropriate performances can be designed [29]. In aerospace applications, polymers are widely employed in several fields, e.g. adhesives, coatings, gaskets, space suites, Multi-Layer Insulation (MLI) [29-31].

On the other hand, the requests for material selection for space environment are challenging: the aggressive orbital environment imposes an accurate design of the components to contrast damaging factors. Extreme temperatures cause thermal curing and degradation, when high, and fragilization, when low; wide thermal cycles imply thermal fatigue and decohesion; atomic oxygen (AO) aggression involves oxidation of surfaces with loss of material and contamination; high vacuum produces outgassing; radiations from Sun and cosmic rays induce cross-linking and degradation; space debris, which could impact on surfaces, cause perforation [32-34]. In addition, inflatable applications require the polymeric material to be resistant, flexible and not porous.

Since no polymers for inflatable applications could withstand all the damaging factors in space environment [29], composite materials are considered. This solution allows to combine several material properties, leading to an optimized design in terms of weight and performances. For inflatable robotic arm applications, the employment of coated fabrics has several advantages: fabrics offer structural stiffness and strength, while coating assure pneumatic insulation and protection of the fibers.

Common fibers adopted in space industry are aramid, liquid crystals, and PE, while coatings could be silicones, urethanes, polyesters and vinyles [29, 30]. Aramids offer good mechanical, thermal and radiation resistance, while they are vulnerable to outgassing; liquid crystals are quite resistant but are sensible to radiations; ethylene is a good trade-off between mechanical, thermal, radiation and outgassing resistance. Thermoplastic-polyurethane (TPU) is resistant to thermal, AO, radiation and outgassing effects; chloroprene presents comparable overall performances, but lower mechanical properties than TPU [35]; vinyl-chlorides like PVC are less resistant to radiations, AO and extreme temperatures, however their wide availability, lightweight and mechanical properties make them a good compromise for preliminary prototypes.

III. Robotic System

The robot consists in two inflatable links and three revolute joints actuated by electric motors. The structure of the extended configuration is shown in Fig.1.

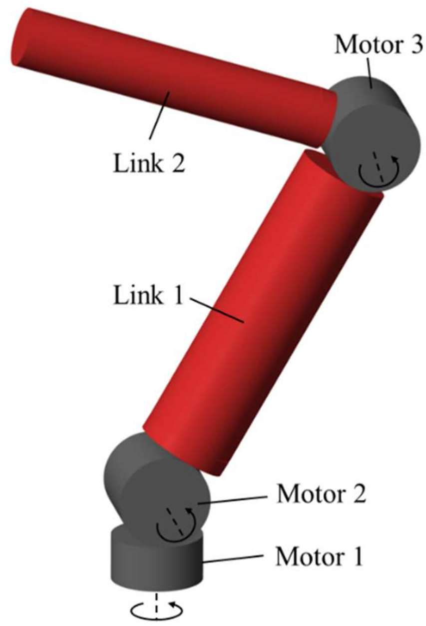

Fig. 1. Schematic representation of the inflatable robot concept. Grey cylinders stand for the joints with electric motors and red parts stand for the inflatable links.

The links have cylindrical shape and are made of a soft material fixed to rigid cups that are connected to the joints. They are designed according to considerations discussed in the following about the influence of the internal pressure and the radius on the performances.

The joints consist of a structural part, that includes the motors. They will be manufactured throughout additive manufacturing techniques after a topological optimization design process that minimizes the weight, guaranteeing the resistance to loads at the same time.

The system includes a pneumatic line, responsible of the deployment phase. Once reached the deployed configuration, the pneumatic supply is cut off and the robot is ready for the working phase.

A. Pneumatic line

A pneumatic line is designed to control the inflation and deflation stages. It consists in a pressurized tank, a reducing valve and two digital valves for each link. Some pressure gauges are expected to be positioned in critical points, e.g. the tank, after the reducing valve and inside the links. The system is shown in Fig. 2.

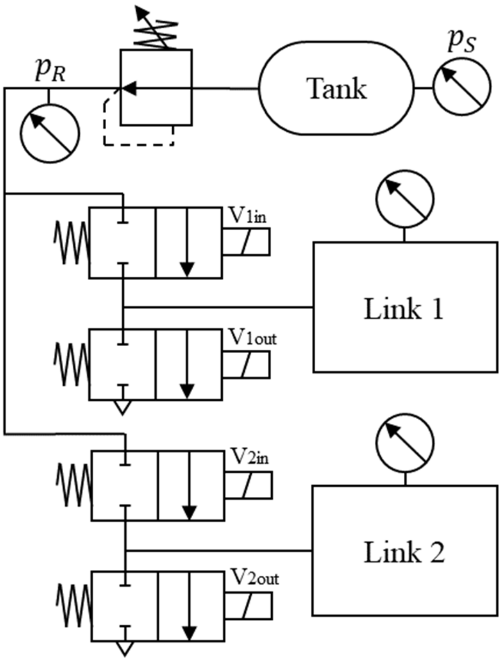

Fig. 2. Scheme of the pneumatic line, consisting of tank, reducing valve, four digital normally closed valves, pressure gauges and links.

The tank is made of composite materials to reduce its weight. Since the tank can admit pressure of $p_S = 30$ MPa and links can show acceptable performance when pressure is higher than 10 kPa, the tank bulk is limited in relation to the dimension of the robot. Additional details about the influence of pressure will be provide in the following.

The pressure p_S of the tank is regulated by a pressure reducing valve to the desired value p_R for the links. Moreover, having no requirements about the needed time for the inflation and deflation stages, small dimension digital valves can be selected. The valves are normally closed to ensure energy savings, as they are active only during the deployment or deflation phase. Each link is connected with a couple of valves. These valves allow the links to be isolated from the pneumatic line, inflated or deflated independently. As clarified in Fig. 2, the nomenclature, e.g. V_{1in}, of the valves allows to identify the link they are referred to (1 or 2) and the role they have when activated: "in" if they permit the inflation and "out" the deflation.

B. Deployment

The possibility to inflate and deflate the robot allows to include it in a small box. The latter contains the robotic system when the links are in their deflated configuration. In Fig. 3 the stages of the deployment and withdrawing phases are presented. Fig. 3a shows how links and joints are arranged inside the box, and Fig. 3c represents the robot in its working configuration. Thanks to the flexibility of the material, the links can be wound around the shaft of the joint, so that the resulting volume is essentially the one of the joints. As the robot is conceived to have long links and compact joints, so that long distances can be reached, the dimensions of the box would be around the 20% of the size of the robot in its deployed configuration.

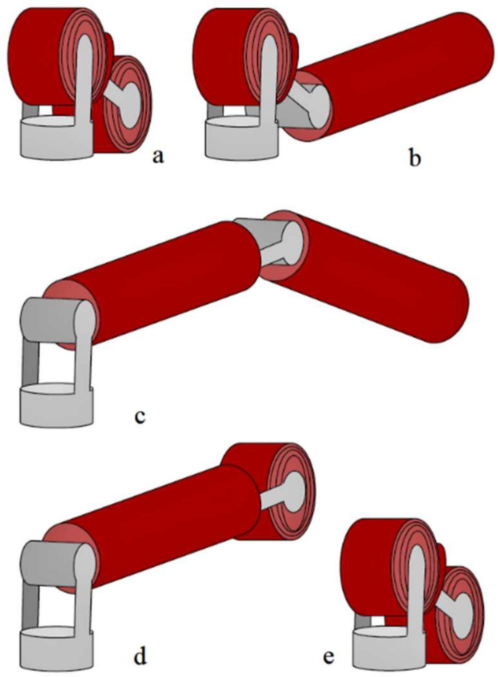

Fig. 3. Scheme of the stages for the deployment and withdrawing phases. a) deflated and retired configuration of the robot before inflation; b) first stage of the inflation phase; c) extended configuration; d) first stage of the withdrawing phase; e) deflated and retired configuration after deflation.

The deployment of the robot from the box is articulated in the following stages:

- In the starting configuration (Fig. 3a), link 1 and link 2 are deflated and wound around the shafts of joint 2 and joint 3, respectively.
- The link 2 is unrolled through the action of the motor of the joint 3, and it is inflated with the air supply, activating the valve V_{2in}, to assume the deployed form (Fig. 3b).
- Subsequently, the link 1 is unwound utilizing the motor 2 and inflated (Fig. 3c), commuting the valve V_{1in}.

After the deployment phase, the robot reaches its working configuration (Fig. 3c). When the withdrawing of the robot is necessary, the following steps are expected:

- The link 2 is deflated, through the commutation of the valve V_{2out}, and rolled around the shaft of the joint by using the motor 3 (Fig. 3d).
- Then, the link 1 is deflated activating the valve V_{1out}, and rolled around the shaft through the motor 2. (Fig. 3e)

The robot comes back to its starting configuration and can be stored in the box.

The motors that enable to wind and unwind the links around the shaft are the same used for controlling the robotic arm.

IV. ELASTOSTATIC MODEL

The system is considered as an anthropomorphic soft arm, consisting of two inflatable links and three joints. In this section the links are assumed pressurized. The links are considered as pseudo-rigid bodies, as in Fig. 4. Each cylindrical link is modelled as two rigid bodies with length l_1 and l_2, connected by a torsional spring, described by the linear relation:

$$k\vartheta = \tau \tag{1}$$

where k is the spring stiffness, ϑ the angular deflection and τ the reaction torque.

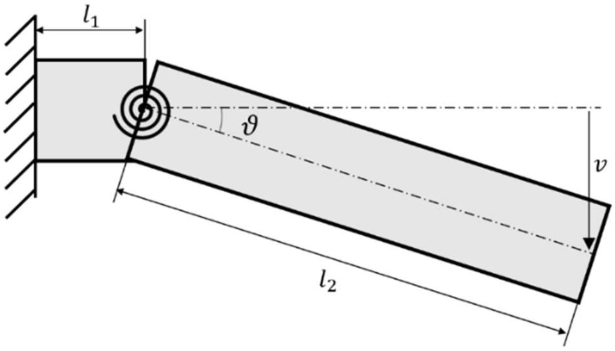

Fig. 4. Inflatable link pseudo-rigid body model, 2D scheme.

As the air pressure maintains the link walls stressed, the model described is a valid approximation of the link behavior. However, it is possible to define the wrinkling moment as the bending load for which the first wrinkles appear. When the structure reaches the wrinkling moment an increase in deflection is obtained without a significant increase in the moment reaction.

In literature, several formulations are proposed for the wrinkling moment estimation [36]. In this work, the following formulation [37] is used to estimate the wrinkling moment M_w:

$$M_w = \frac{\pi}{4}\pi p r^3 \tag{2}$$

where p is the differential pressure between the inner and outside part of the link, and r is the radius.

The inflatable link model evaluates the deflections along two orthogonal axes, neglecting torsional deformations. Therefore, two virtual torsional springs are considered for each link. The robotic arm, with the introduction of the pseudo rigid body model for the inflatable links, reaches 7 degrees of freedom: 3 for the actuated joints and 2 for each link introduced by the virtual springs.

V. EXPERIMENTAL CHARACTERIZATION

An experimental campaign was carried out to validate the model and develop a methodology to characterize an inflatable link. The experimental set-up and the prototype are shown in Fig. 5. The link prototype is manufactured using a soft PVC reinforced foil, folded over itself to obtain a pipe and fixed by using glue. The extremities are closed with two rigid PVC caps and fixed with seals and metallic bands.

The link is fixed to a dedicated support and considered as cantilever. A UR5 robot, equipped with a force sensor and a custom probe, is used to deflect in a precise and repeatable way the link. Then, a map with deflections and applied forces is built. The pressure is maintained constant during the test using a pressure regulator and measured using a pressure sensor.

The tests are performed on a link with 55 mm of radius and 600 mm long, using pressure values in the range 10 – 60 kPa.

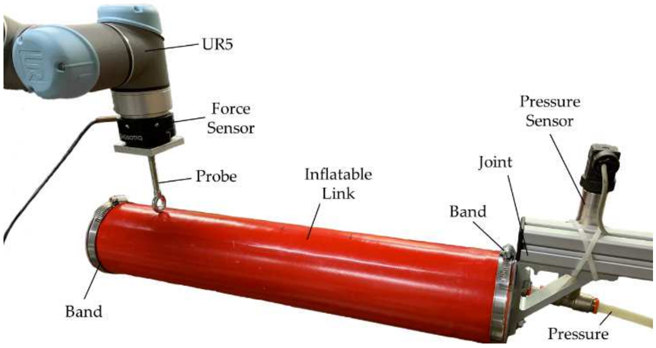

Fig. 5. Experimental set-up for inflatable link characterization using a collaborative robot.

VI. RESULTS

The experimental tests have been post-processed to deduce the static characteristic of the inflatable link. In Fig. 6 the experimental data of a specific test, are shown, underling the characteristic function between the angular deformation and the applied torque. Results refer to a test with the pressure of the link set at 20 kPa. The following considerations can be considered valid for all the tests. The theoretical wrinkling moment M_w is shown.

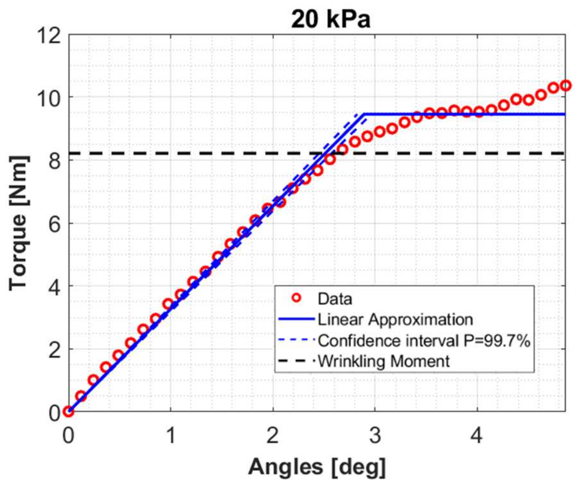

Fig. 6. Experimental results and linear regression approximation of the test of the inflatable link pressurized at 20 kPa.

The trend of the points below the wrinkling moment level can be considered linear, so a linear regression is performed. As the points over the wrinkling moment level show an asymptotic tendency that highlights the link inability to support greater loads, in a simplified way a saturation is assumed. The saturation level M_{max} has been calculated by average of the moment values of the remaining points.

The linear regression permits to evaluate the virtual spring stiffness k for each test at different pressures. Results shown in Table 1 suggest there is not an evident dependency of the bending stiffness k on the pressure in the investigated range. On the contrary the pressure establishes the maximum moment the structure can held. The trend of the calculated maximum torque and theoretical wrinkling moments is comparable.

TABLE I. STIFFNESS AND MAXIMUM MOMENT ESTIMATION

p **(kPa)**	***k*** **(Nm/rad)**	M_{max} **(Nm)**	M_w **(Nm)**
10	183	5.0	4.1
20	187	9.5	8.2
30	156	15.0	12.3
40	174	18.8	16.4
50	169	21.8	20.5
60	167	N/A	24.6

In Fig. 7, an example of wrinkle onset is shown. The winkles occur in the weakest region of the link, due to the application of the external force that results in a bigger moment than the wrinkling moment M_w.

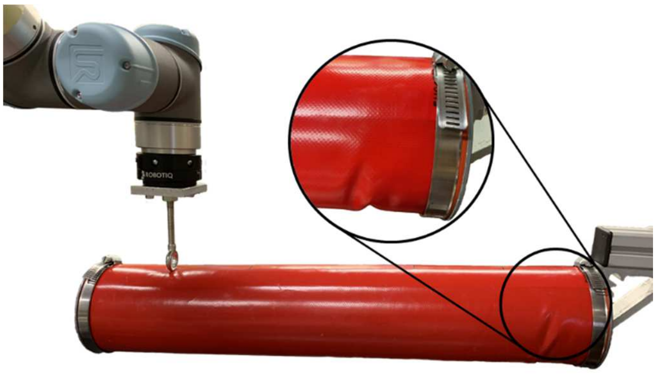

Fig. 7. Example of appearance of wrinkles during the tests. In the enlargement in evidence, it is shown the winkles from a different perspective.

VII. DISCUSSION

Results demonstrate that the links have a linear behavior in terms of deflection when they are exposed to a lower moment than the wrinkling moment M_w. Equation (2) effectively predicts the wrinkling moment and the limit of the linear characteristic of the links. Assuming to define as working conditions for the robot the range in which wrinkles are absent, (2) allows to determine the trade-off for the payload, the dimensions of the links and the pressure necessary for the inflation.

A first prototype of the robot, for laboratory testing, so considering the presence of gravity, will be built using, as link 2, the link used in the experiments of the present paper having radius of 55 mm and, as link 1, a link with the same length and radius of 85 mm. With this configuration, setting a relative pressure of 30 kPa, the robot could support a payload of 2 kg. The manufacturing of the link will avoid the use of seals and metallic bands to move to a simpler solution with caps fixed by glue, guaranteeing a more feasible air isolation and stress resistance, although renouncing to the versatility in terms of assembly easiness of the current solution.

For aerospace applications, assuming the length of the links of 5 m, a force of 5 N applied through the tool center point, an absolute pressure of 30 kPa, and considering slow motion in the space, the radius of links 1 and 2 should be 80 mm and 100 mm, respectively, in a conservative design.

VIII. CONCLUSIONS

This paper presented a novel concept of a deployable robotic arm with two inflatable links and three electric motors. The robot proposed is meant to be enclosed in a package and deployed only when necessary. In its working configuration, the robot is disconnected from air supply.

A review of possible materials to be used for the inflatable links was performed underlining the critical aspects. The deployment and withdrawing strategies were discussed, assuming precise geometrical features of the joints and the use of electric motors. Then, a pseudo-rigid body model is used to describe to behavior of the soft links through an elastostatic approach.

The prototype of the inflatable link was built and statically characterized according to the presented model. Results showed how the supplied pressure determines the maximum torque the link can support, defining the limits of the elastostatic model applicability. Therefore, the wrinkling moment of each link defines the working conditions for the robot, defining the design criteria for the development of the first prototype.

Further works should investigate the dynamic behavior of the links, develop the prototype of the overall system, and validate the deployment strategy. In addition, control algorithms should be implemented, using built-in sensors as Inertial Motion Units (IMU), flex sensors, or computer vision and sensor fusion strategies.

REFERENCES

[1] C. Feifei, M. Y. Wang. “Design Optimization of Soft Robots: A Review of the State of the Art.” IEEE Robotics & Automation Magazine, 2020, vol. 27(4), pp. 27-43.

[2] G. Methenitis, D. Hennes, D. Izzo, A. Visser. “Novelty search for soft robotic space exploration.” In Proceedings of the 2015 annual conference on Genetic and Evolutionary Computation, Madrid, Spain, 2015.

[3] G. E Fenci, N. G. Currie. “Deployable structures classification: A review.” International Journal of Space Structures, 2017, vol. 32(2), pp. 112–130.

[4] J. Hughes, U. Culha, F. Giardina, F. Guenther, A. Rosendo, F. Iida. “Soft Manipulators and Grippers: A Review.” Frontiers in Robotics and AI, 2016, vol. 3.

[5] D. Cadogan, C. Sandy, M. Grahne. “Development and evaluation of the mars pathfinder inflatable airbag landing system.” Acta Astronautica, 2002, vol. 50(2), pp. 633–640.

[6] R.E. Freeland, G.D. Bilyeu, G.R. Veal, M.D. Steiner, D.E. Carson. "Large Inflatable Deployable Antenna Flight Experiment Results." Acta Astronautica, 1997, vol. 41(4), pp. 267-277.

[7] G. T. Williams, P. K. Malone, F. J. Jankowski, G. J. Jr. Vendura. "Developing an Inflatable Solar Array." Developing an Inflatable Solar Array, 1992.

[8] L. Puig, A. Barton, N. Rando. “A review on large deployable structures for astrophysics missions.” Acta Astronautica, 2010, vol. 67, pp. 12–26.

[9] M. E. Giannaccini, C. Xiang, A. Atyabi, T. Theodoridis, S. Nefti-Meziani, S. Davis. "Novel Design of a Soft Lightweight Pneumatic Continuum Robot Arm with Decoupled Variable Stiffness and Positioning." Soft Robotics, 2018, vol. 5(1), pp. 54-70.

[10] H-J. Kim, A. Kawamura, Y. Nishioka, S. Kawamura. "Mechanical Design and Control of Inflatable Robotic Arms for High Positioning Accuracy." Advanced Robotics, 2018, vol. 32(2), pp. 89-104.

[11] R. Mengacci, F. Angelini, M. G. Catalano, G. Grioli, A. Bicchi, M. Garabini. “On the motion/stiffness decoupling property of articulated soft robots with application to model-free torque iterative learning control.” The International Journal of Robotics Research, 2020.

[12] J. M. Alvarez Palacio, A. Riwan, N. Mechbal, E. Monteiro, S. Voisembert. "A Novel Inflatable Actuator for Inflatable Robotic Arms." 2017 IEEE International Conference on Advanced Intelligent Mechatronics (AIM), Munich, 2017, pp. 88-93.

[13] J. Walker, T. Zidek, C. Harbel, S. Yoon, F. S. Strickland, S. Kumar, M. Shin. “Soft Robotics: A Review of Recent Developments of Pneumatic Soft Actuators.” Actuators, 2020, vol. 9(1).

[14] X. Li, K. Sun, C. Guo, T. Liu, H. Liu. "Design, Modeling and Characterization of a Joint for Inflatable Robotic Arms." Mechatronics, 2020, vol. 65.

[15] G. Martius, R. Hostettler, A. Knoll, R. Der. "Compliant control for soft robots: Emergent behavior of a tendon driven anthropomorphic arm." 2016 IEEE/RSJ International Conference on Intelligent Robots and Systems (IROS), Daejeon, 2016, pp. 767-773.

[16] M. T. Gillespie, C. M. Best, M. D. Killpack. "Simultaneous position and stiffness control for an inflatable soft robot." 2016 IEEE International Conference on Robotics and Automation (ICRA), Stockholm, 2016, pp. 1095-1101.

[17] A. De Luca, W. Book. “Robots with Flexible Elements”. In Springer Handbook of Robotics, Siciliano B., Khatib O.; Eds; Springer, Berlin, Heidelberg, 2016, pp. 243-282.

[18] S. Sanan, J. B. Moidel, C. G. Atkeson. "Robots with Inflatable Links." 2009 IEEE/RSJ International Conference on Intelligent Robots and Systems, St. Louis, MO, 2009, pp. 4331-4336.

[19] J. Oliveira, A. Ferreira, J. C. P. Reis. "Design and Experiments on an Inflatable Link Robot with a Built-in Vision Sensor." Mechatronics, 2020, vol. 65.

[20] L. S. Scimmi, M. Melchiorre, S. Mauro and S. P. Pastorelli, "Implementing a Vision-Based Collision Avoidance Algorithm on a UR3 Robot," 2019 23rd International Conference on Mechatronics Technology (ICMT), 2019, pp. 1-6, doi: 10.1109/ICMECT.2019.8932105.

[21] M. Melchiorre, L. S. Scimmi, S. P. Pastorelli and S. Mauro, "Collison Avoidance using Point Cloud Data Fusion from Multiple Depth Sensors: A Practical Approach," 2019 23rd International Conference on Mechatronics Technology (ICMT), 2019, pp. 1-6, doi: 10.1109/ICMECT.2019.8932143.

[22] V. A. Sujan, S. Dubowsky. "Design of a Lightweight Hyper-Redundant Deployable Binary Manipulator ." ASME. J. Mech. Des. 2004, vol. 126(1), pp. 29-39.

[23] G. Kiper and E. Soylemez, "Deployable space structures," 2009 4th International Conference on Recent Advances in Space Technologies, 2009, pp. 131-138, doi: 10.1109/RAST.2009.5158183.

[24] E. Gdoutos, A. Truong, A. Pedivellano, F. Royer, S. Pellegrino. "Ultralight Deployable Space Structure Prototype." AIAA Scitech 2020 Forum. January 2020.

[25] H. Furuya, S. Murata, M. Nakahara, D. Jodoi, Y. Terada, K. Takadama. "Concept of Inflatable Tensegrity for Large Space Structures." 47th AIAA/ASME/ASCE/AHS/ASC Structures, Structural Dynamics, and Materials Conference, May 2006.

[26] J. Wei, H. Tan, W. Wang, and X. Cao. “Deployable Dynamic Analysis and On-Orbit Experiment for Inflatable Gravity-Gradient Boom.” Advances in Space Research, 2015, vol. 55(2), pp. 639-46.

[27] M. Schenk, A. D. Viquerat, K. A. Seffen, S. D. Guest. “Review of Inflatable Booms for Deployable Space Structures: Packing and Rigidization.” Journal of Spacecraft and Rockets, 2014.

[28] M. Troise, M. Gaidano, P. Palmieri, and S. Mauro, “Preliminary Analysis of a Lightweight and Deployable Soft Robot for Space Applications,” Applied Sciences, vol. 11, no. 6, p. 2558, Mar. 2021.

[29] C. M. Jenkins, “Gossamer Spacecraft, Membrane and Inflatable Structures Technology for Space Applications”, Progress in Astronautics and Aeronautics, 2001.

[30] P. B. Willis, C.-H. Hsieh, “Space Applications of Polymeric Materials”, Kobunshi, 2000, vol. 49.

[31] W. J. Larson, J. R. Wertz, “Space Mission Analysis and Design”, Microcosm, 1999.

[32] J. Chen, N. Ding, Z. Li, W. Wang, “Organic polymer materials in the space environment”, Progress in Aerospace Sciences, 2016, vol. 83.

[33] E. Grossman, I. Gouzman, “Space environment effects on polymers in low earth orbit”, Nuclear Instruments and Methods in Physics Research Section B: Beam Interactions with Materials and Atoms, 2003, vol. 208.

[34] R. Pastore, A. Delfini, M. Albano, A. Vricella, M. Marchetti, F. Santoni, F. Piergentili, “Outgassing effect in polymeric composites exposed to space environment thermal-vacuum conditions”, Acta Astronautica, 2020, vol. 170.

[35] Michael Rivera, “Elastomers in space and in other high vacuum environments”, Rubber Chemistry and Technology, 1966.

[36] S. L. Veldman, O. K. Bergsma, A. Beukers. "Bending of Anisotropic Inflated Cylindrical Beams." Thin-walled Structures. 2005, vol. 43(3), pp. 461-75.

[37] C. Wielgosz, JC. Thomas. “Deflections of inflatable fabric panels at high pressure.” Thin-Walled Struct. 2002, vol. 40(6), pp. 523-536.